Pressure Effect in the Atomic Distribution in Liquid Helium by Neutron Diffraction

D. G. HENSHAW
Division of Physics, Atomic Energy of Canada Limited, Chalk River, Ontario, Canada
(Received January 18, 1960)

The angular distribution of 1.06_4 A neutrons scattered from liquid helium at temperatures and pressures in the range 1.2°K to 4.24°K and 0 to 51.3 atmospheres for densities up to 0.184 gram/cc has been measured at about 210 equally spaced points in the angular range 5° to 62°. With increasing liquid density, the principle maximum moves to larger angles and increases in height. The liquid structure factors are given for densities of 0.166 gram/cc and 0.184 gram/cc. The density distribution functions are deduced for each of the scattering patterns. A study of these gives 2.27±0.08 A as the nearest distance of approach of two atoms in the liquid. The number of neighbors under the first and second coordinate shells changes from about 6.5 to 8.5 atoms and from about 9 to 5.5 atoms, respectively, for density changes from 0.095 gram/cc to 0.184 gram/cc. The corresponding change in the ratio of their spacings is from 1.47_5 to 1.38, which values are close to $\sqrt{2}$, the theoretical ratio for a close packed lattice. The analysis shows that the density changes in the liquid and during the solid-liquid transformation cannot be accounted for on the basis of a uniform dilation of a basic structure. The changes in the distribution function caused by pressure are different from those caused by temperature along the normal vapor pressure line.

INTRODUCTION

THE density distributions in liquids may be determined by transforming the angular distributions of coherently scattered radiations and they yield information about the spatial order in the liquid. In the case of liquid helium, such measurements have been made using neutrons[1,2] and x rays[3–7] for the liquid under its normal vapor pressure. For these conditions, the change in the atomic density distribution with liquid density is small. Both neutron[1,2] and x-ray[3] scattering have shown that there is a change in the scattering pattern associated with λ transition which indicates that the liquid below the λ point has lower spatial order than just above.

In the present work the angular distribution of 1.06_4 A neutrons has been measured for liquid helium at several densities up to 0.184 gram/cc by applying pressures up to 51.3 atmospheres to the liquid. The scattering patterns were transformed to the radial distribution functions. The changes in the scattering patterns and distribution functions are discussed in relation to the change in liquid density, the change in density during the solid-liquid transformation and the λ transition, and in relation to the distribution functions previously measured[1] for the liquid under its normal vapor pressure.

APPARATUS

The angular distributions of scattered neutrons were measured with the Chalk River Neutron Spectrometer.[8]

The specimens of liquid helium were held in the liquid helium cryostat.[1] The scattering chamber, modified as shown in Fig. 1, consisted in a 1-in. diameter Dural cassette having walls 0.065-in. thick for a height of $2\frac{1}{2}$-in. at the level of the neutron beam. This cassette was sealed to the face of the liquid helium chamber by means of indium. A $\frac{5}{8}$-in. diameter bar of aluminum on the upper end of the cassette extended into the liquid helium for a distance of 10 in. in order to ensure good thermal contact between the liquid and the cassette. A resistor[9] cemented into the cassette was used as a temperature sensitive element and calibrated using the bulb of the cassette as a vapor pressure thermometer. The cassette was connected to the high-pressure helium supply by means of a $\frac{1}{8}$-in. diameter, 0.005-in. thick wall nickel silver tube, one end of which was hard soldered to the base of the cassette; the other entered the vacuum system of the cryostat through the top cover plate and was soldered to a liquid nitrogen and helium chamber for thermal insulation. Radiation shields attached to the liquid helium and nitrogen chambers were used to insulate the cassette thermally. A cylinder[10] of helium gas was used as the source of high-pressure helium. The pressure of the liquid in the cassette was measured using a 0–2000 psi Bourdon type gauge with 10 psi subdivisions. The capacity of the liquid helium chamber was 6 liters. It was possible to make measurements for periods up to 72 hours and 24 hours with the liquid helium at 4.2°K and 1.5°K, respectively.

MEASUREMENTS

The angular distributions of 1.06_4 A neutrons scattered by specimens of liquid helium at the series of temperatures and pressures in the range 1.2°K to 4.24°K

[1] D. G. Hurst and D. G. Henshaw, Phys. Rev. **100**, 994 (1955).
[2] D. G. Henshaw, preceding paper [Phys. Rev. **119**, 9 (1960)].
[3] J. Reekie and T. S. Hutchison, Phys. Rev. **92**, 827 (1953).
[4] T. S. Hutchison, C. F. A. Beaumont, and J. Reekie, Proc. Phys. Soc. (London) **A66**, 409 (1953).
[5] C. F. A. Beaumont, and J. Reekie, Proc. Roy. Soc. (London) **A228**, 363 (1955).
[6] W. L. Gordon, C. H. Shaw, and J. G. Daunt, Phys. Rev. **96**, 1444 (1959).
[7] W. L. Gordon, C. H. Shaw, and J. G. Daunt, J. Phys. Chem. 1444 (1959).
[8] D. G. Henshaw, Phys. Rev. **111**, 1470 (1958); preceding paper [Phys. Rev. **119**, 9 (1960)].
[9] J. R. Clement and E. H. Quinnel, Rev. Sci. Instr. **23**, 213 (1952).
[10] This gas was supplied by the Matheson Company Incorporated, East Rutherford, New Jersey, U. S. A.

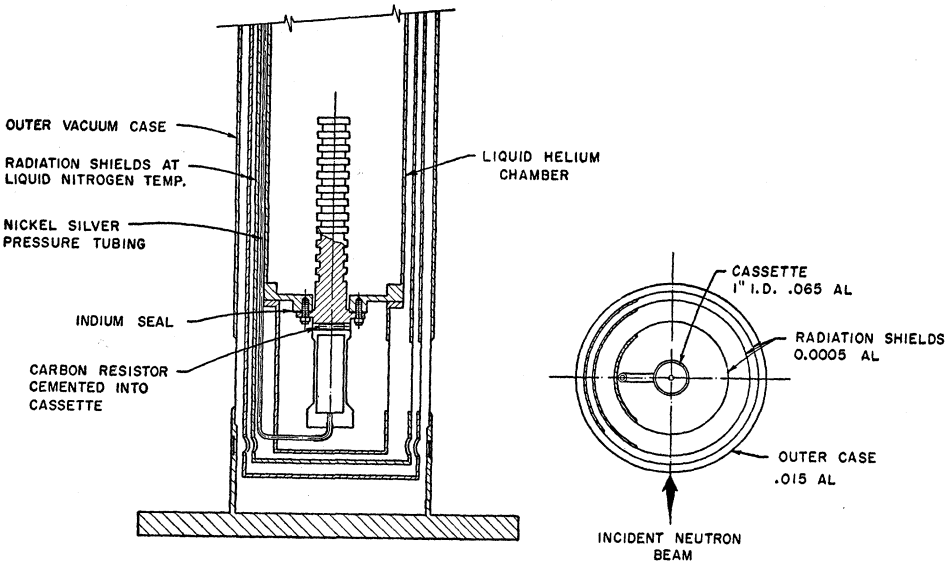

FIG. 1. The cassette used as a scattering chamber to hold the specimens of liquid helium at pressures up to 75 atmospheres. The solid aluminum extension was used to insure good thermal contact between the specimen and the liquid helium used as the refrigerant. The carbon resistor was used as a temperature-sensitive element.

and 0 to 51.3 atmosphers, listed in Table I, were measured over the angular range 5° to 62°. These measurements were made at several pressures at a constant temperature of 4.2°K and at several temperatures and pressures at a density of about 0.17 gram/cc. The background from the evacuated cassette was measured at 4.2°K. At angles greater than 10°, it was essentially constant between the intense lines associated with the fcc structure of the aluminum cassette and was about 13% of the total scattering at large angles. Below 10°, the background rose continuously and became excessive at angles less than 3°. The background was corrected for the attenuation through the liquid helium using the measured transmission cross section for liquid helium of 0.73 barn[1] before applying it as a correction to the measured curves.

The intensities[11] corrected for background, for counter resolution in the region of the main peak using the measured resolution of 1.3°, and for multiple scattering of neutrons solely in the liquid helium, were computed for each curve. Figure 2 shows the corrected curve for the liquid at 4.2° and 51.3 atmospheres corresponding to a density of 0.184 gram/cc. The horizontal line represents the level of multiple scattering of neutrons in both the liquid and walls of the container corresponding to the value of Δ of Eq. (2) of the accompanying paper and is about 4% of the total scattering at large angles. The curve shows low scattering at small angles, a peak in the region of 21.3° and at large angles an oscillation (with a maximum in the region of 45°) about a scattering level which decreases in much the same way as the scattering from free helium atoms.[1,2]

The statistical accuracy of the measurements is higher in the region 5° to 30° than 30° to 65° and may be estimated from the scatter of the experimental points. The curve is dotted in the region of the intense background lines from the aluminum cassette where the accuracy of the measurements is low. The form of all the curves is similar but they differ in detail. With increasing liquid density, the shape of the main diffraction peak changes while its height increases relative to the large-angle scattering and its position moves to larger angles. The changes in the small-angle scattering were consistent with those expected on the basis of the changes in the zero-angle scattering calculated from the formula

$$L_0 = nkT\chi_T,$$

where L_0 = zero-angle structure factor, n = particle num-

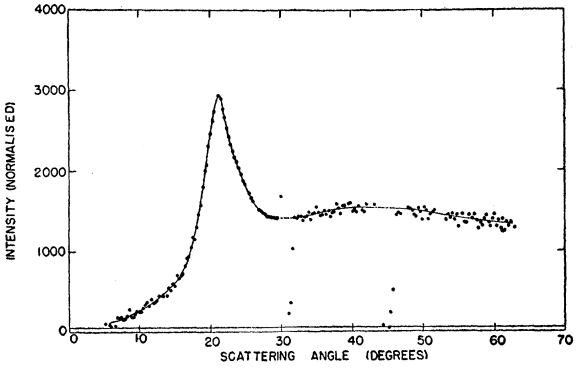

FIG. 2. The angular distribution of 1.06$_4$ A neutrons scattered from liquid helium at 4.2°K and 51.3 atmospheres corresponding to a density of 0.184 gram/cc. The experimental points were corrected for background, counter resolution in the region of the main peak and for multiple scattering in the liquid helium. The scatter of the points (some not shown) in the region of 31°, 44°, and 52° is owing to the large background lines from the aluminum cassette. The horizontal line represents the level of the multiple scattering for neutrons scattered both by the liquid helium and the walls of the cassette.

[11] The method of analyzing the measurements is that given in the preceding paper (reference 2) where the symbols are defined. Equation numbers used here refer to those given in that paper.

TABLE I. The conditions at which the curves were measured, together with the data from which the curves were plotted.

Curve No.	Temperature (°K)	Pressure (atmospheres)	Density (grams/cc)	Height of maximum $(2/\pi)si(s)$ (A^{-1})	Position of maximum $(2/\pi)si(s)$ (A^{-1})	Position of 2nd zero $(2/\pi)si(s)$ (A^{-1})	Position of 3rd zero $(2/\pi)si(s)$ (A^{-1})	Position where $4\pi r\rho(r)$ rises from zero (A)	Position of maximum in $4\pi\rho(r)$ (A)	Number of first neighbors peak symmetrical in $4\pi r\rho(r)$	Number of first neighbors peak symmetrical in $4\pi r^2\rho(r)$	Number of second neighbors	Spacing second maximum (A)
1[a]	5.04	N.V.P.	0.095	0.27	2.05	1.75	2.55	2.20	3.94	7.0	5.8	9.2	5.6
2[a]	4.24	N.V.P.	0.125	0.45	2.07	1.72	2.70	2.25	3.72	8.1	7.0	7.8	5.2
3[a]	2.2	N.V.P.	0.146	0.47	2.07	1.77	2.57	2.25	3.70	8.6	7.4	8.2	5.2
4	4.2	27.2	0.170	0.99	2.15	1.85	2.68	2.35	3.55	8.7	7.8		
5	1.84	21.4	0.171	0.106	2.12_5	1.88	2.70	2.28	3.60	9.8	8.6		
6	2.25	19.8	0.171	0.103	2.15	1.88	2.80	2.20	3.45	7.9	7.0		
7	4.2	51.3	0.184	1.14	2.20	1.93	2.68	2.26	3.55	10.2	8.9	5.7	4.9
8	4.2	27.2	0.170	0.83	2.20	1.88	2.73						
9	4.2	32.0	0.174	0.95	2.20	1.88	2.73	2.25	3.45	7.9	7.0		
10	1.17	21.4	0.169	0.89	2.17_5	1.88	2.78	2.25	3.50	8.3	7.4		
11	4.2	12.4	0.154	0.66	2.12_5	1.85	2.73	2.30	3.75	10.4	9.0		
12	4.2	7.6	0.147_4	0.51	2.10	1.80	2.65						
13	1.95	27.5	0.177_5	1.10	2.17_5	1.90	2.78	2.35	3.60	7.6	6.8		
14	2.05	15.0	0.166	0.98	2.15	1.85	2.65	2.35	3.60	9.2	8.1	5.5	4.9
15	2.06	7.8	0.157_5	0.73	2.10	1.83	2.70						
16	2.2	23.1	0.171	0.96	2.15	1.88	2.70	2.25	3.45	7.6	6.8		

[a] These data have been taken from reference 1.

ber density, T = liquid temperature, and χ_T = isothermal compressibility.

ANALYSIS OF MEASUREMENTS

To compare the measured curves, it is necessary that they be normalized. Suitable functions[11] for their comparison are $i(s)+1$ and $(2/\pi)si(s)$. The function $i(s)$ was deduced for each of the measured curves by plotting the corrected intensities against angle. Smooth curves were drawn through the points and extrapolated to the calculated zero-angle scattering. The intensities read from the smooth curves in steps of $0.1s$ for $0 \leq s \leq 6.0$ A^{-1} were used to compute the function $i(s)$ of Eq. (2). The value of I_∞ was chosen to satisfy Eq. (3) while Δ was determined by calculating[12] the transforms $r\rho(r)$ for spacings out to 3.0 A for several values of Δ. The value of Δ used was that which made the average value of $r\rho(r)=0$ for spacings out to 2.3 A and was about 4% of the total scattering at large angles. The error in determining $i(s)$ arises mainly from the error in the determination of I_∞ which depends in large part on the scattering at large s owing to the s^2 relation in Eq. (3). The error in the determination of I_∞ is estimated to be $\pm 3\%$ from which the error in the determination of $i(s)$ may be estimated. In the region of the peak where $i(s)$ is about 0.7, the corresponding errors would be ∓ 0.06. The relative error between the curves is less than this because of the consistency in their treatment.

The function $i(s)+1$, the liquid structure factor, has been plotted in Fig. 3 for the liquid at densities of 0.184 gram/cc (4.2°K and 51.3 atmospheres) and 0.166 gram/cc (2.05°K and 14.9 atmospheres). Each curve

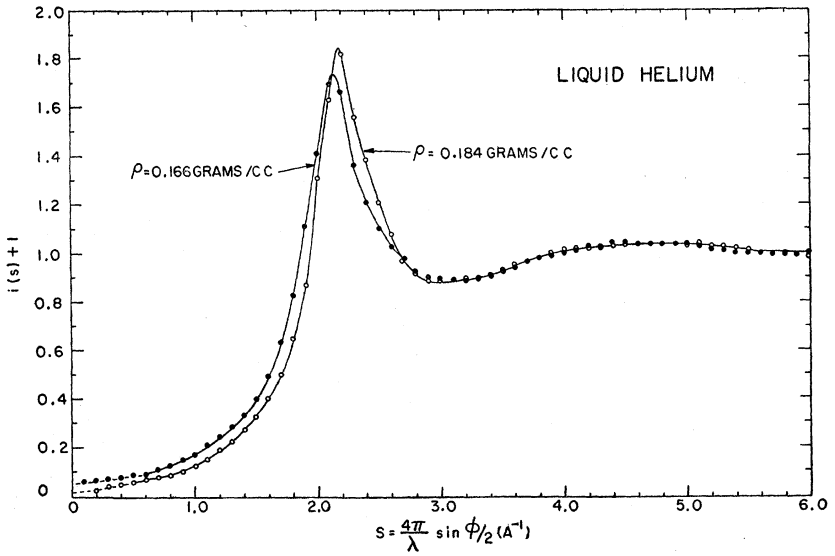

FIG. 3. The liquid structure factor $i(s)+1$ for the liquid helium at 0.184 gram/cc and 0.166 gram/cc corresponding to 4.2°K and 51.3 atmospheres and 2.05°K and 74.9 atmospheres, respectively. These functions were deduced from smooth curves drawn through the corrected experimental points as described in the text.

[12] The Fourier transforms were calculated at the Computation Center, University of Toronto, on FERUT.

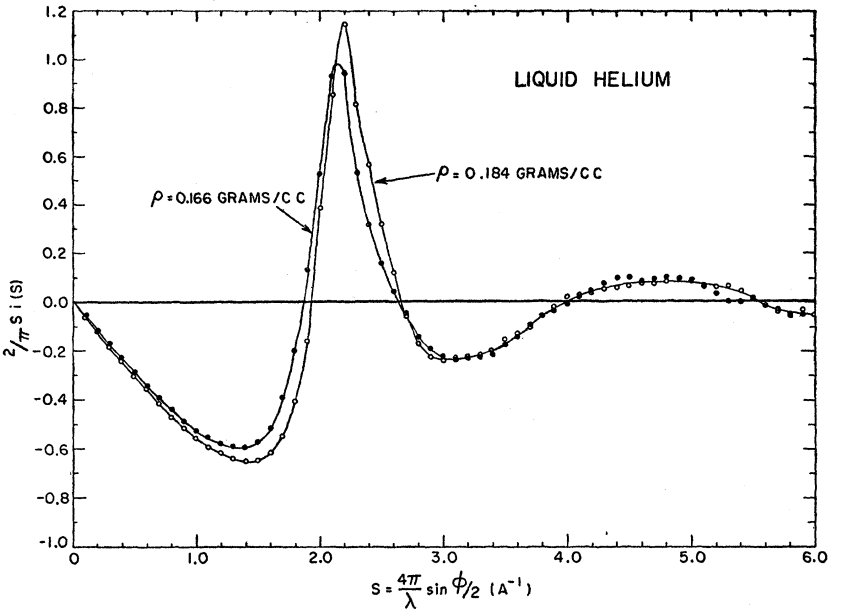

FIG. 4. The function $(2/\pi)si(s)$ corresponding to each of the structure factor curves of Fig. 3.

shows low values at small s, a peak in the region of $s=2.15$ A^{-1} and at large s an oscillation about unity with a minimum and second broad maximum in the region of 3.0 A^{-1} and 4.7 A^{-1}, respectively, which are 12% and 3% below and above the mean value at large s. Within experimental error there are no differences between the curves for s greater than 3.0 A^{-1}. The function $i(s)+1$ for the higher liquid density lies below and above the lower density curve for values of s less and greater than 2.14 A^{-1}, respectively. At the higher density, the peak is higher and at a larger value of s than at the lower density. Thus density changes induced by pressure cause much more marked changes in the height and position of the maximum than are observed for the liquid under its normal vapor pressure.[1]

The function $(2/\pi)si(s)$ used in the transformation was the more suitable for the comparison of the curves and is shown plotted in Fig. 4 for each of the curves of Fig. 3. The form of the main diffraction peak is defined by the height and position of the main maximum together with the positions of its zeros. They have been listed in Table I for each of the measured curves and have been plotted in Figs. 5 and 6, respectively, as a function of liquid density. The theoretical variations of these parameters assuming a uniform dilation of a basic structure (see Appendix I) are shown by the smooth curves. The experimental points do not fall on the theoretical curves and thus indicate that the density changes in the liquid cannot be accounted for on the basis of such a simple model and that they are considerably more complex in nature. In the region of $\rho=0.170$ gram/cc, the variation of peak height with density is almost linear. The heights of the maxima of the curves having densities in the region of 0.170 gram/cc were normalized to this density assuming this linear relationship and plotted as a function of temperature in Fig. 7 together with their estimated errors to determine whether or not there is any temperature variation of this parameter. The vertical arrow represents the λ temperature corresponding to this density. Examination of the figure shows that the height of the peak at 1.15° is 0.90 and is lower than 0.98 the average of the heights at and above the λ point. At 4.2°K there is considerably more scatter of the points. The lowest value has been shown

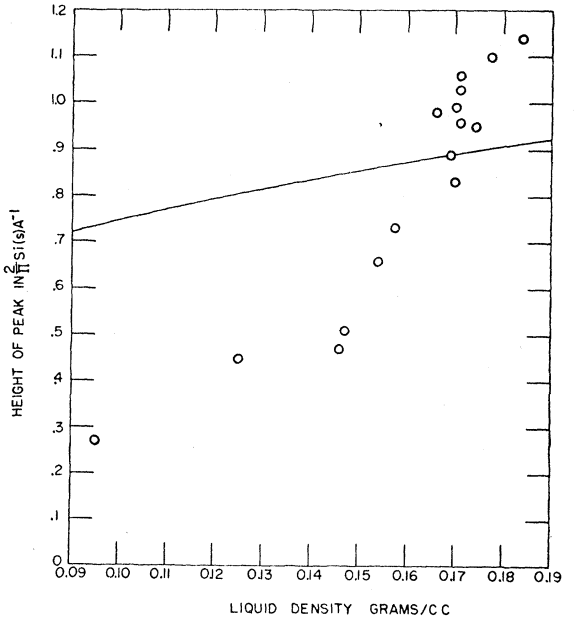

FIG. 5. The height of the maximum in $(2/\pi)si(s)$ plotted as a function of liquid density. The smooth curve shows the expected variation assuming a uniform dilation of a basic structure. The experimental points do not fall on the theoretical curve.

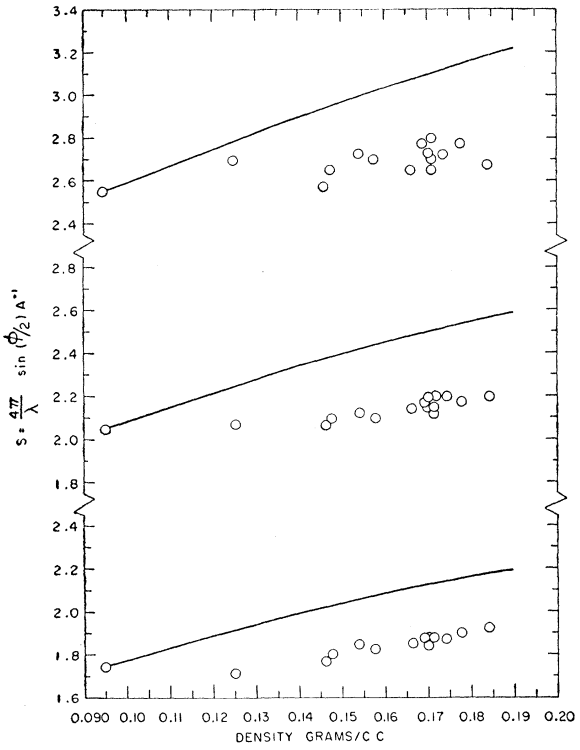

FIG. 6. The lower, middle, and upper sets of points are the positions of the 2nd zero, the maximum, and the 3rd zero of $(2/\pi)si(s)$ as a function of liquid density. The smooth curve gives the expected variation on the basis of a uniform dilation of a basic structure. The experimental points do not fit the theoretical curves.

with a larger estimated error because the measurements were made with lower accuracy. Allowing for this the average value in this region is 0.94. Although the change in peak height is not outside experimental error, these results suggest that there may be a change associated with the λ transition. The ratio of the peak height above (in the region of 2°K) to below (1.15°K) the λ point is 1.09±0.07 which may represent a significant change associated with the λ transition and this may be compared with the ratio[13] 1.14 for the change[2] measured for liquid helium under its normal vapor pressure. These results then suggest that there is a change in the scattering patterns owing to the λ transition which would indicate lower spatial order in the liquid below the λ point than above which is consistent with the behavior found for the liquid under its normal vapor pressure.[1,2,7]

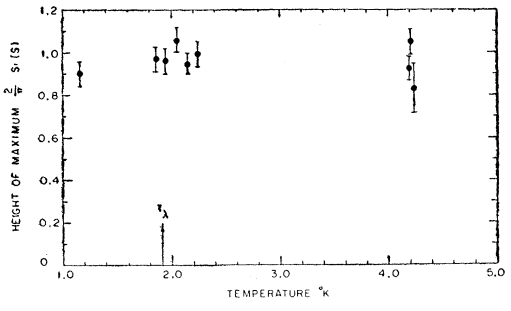

FIG. 7. The height of the maximum in $(2/\pi)si(s)$ at constant density as a function of temperature. Each point has been normalized to a density of 0.170 gram/cc. The vertical arrow represents the λ temperature at this pressure.

DENSITY DISTRIBUTIONS

The radial distribution functions $4\pi r^2[\rho(r)-\rho_0]$ were calculated for all the curves in steps of 0.1 A for $0 \leq r \leq 20.0$ A. The curves for the liquid at 0.184 gram/cc and 0.166 gram/cc have been plotted in Fig. 8 together with those measured[14] along the normal vapor pressure line at densities of 0.146, 0.125, and 0.095 gram/cc. The

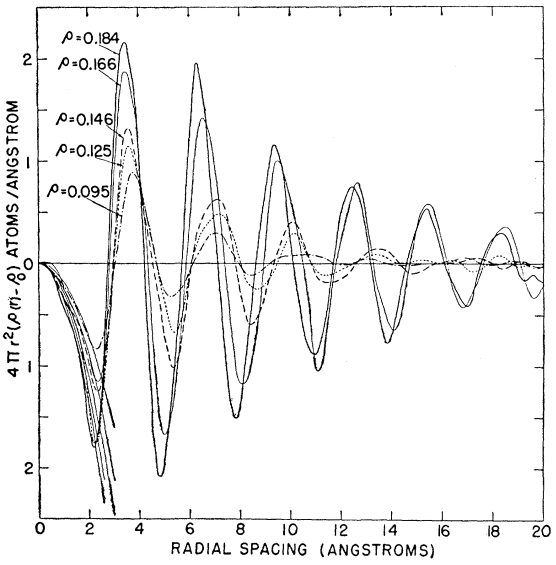

FIG. 8. The transforms $4\pi r^2[\rho(r)-\rho_0]$ for liquid helium at the densities shown. The curves at the higher densities were deduced from the structure factors of Fig. 3 while the three lower curves are for liquid helium under its normal vapor pressure (see reference 1). The parabolic curves are $-4\pi r^2\rho_0$ where ρ_0 is the mean atomic density.

parabolic curves out to about 3 A represent $-4\pi r^2\rho_0$, the negative of the mean atomic density. Each curve shows an oscillation[15] about $-4\pi r^2\rho_0$ for spacings out to 2.3 A, a maximum in the region of 3.5 A and at larger spacings oscillations about zero with an amplitude which decreases with increased radial spacing. Changes in liquid density cause marked changes in the details of the oscillation. With increasing liquid density the amplitudes of the maxima increase while the rate at which these maxima decrease with increasing radial spacing

[13] The ratio of the heights of $(2/\pi)si(s)$ is quoted here while that quoted in reference (2) is $i(s)+1$.

[14] The curves for liquid densities of 0.146, 0.125, and 0.095 gram/cc have been taken from our earlier publication.[1]

[15] As has been discussed earlier,[1,2,10] these oscillations are almost certainly spurious arising from experimental error and the finite range of s over which the measurements were made.

decreases. The spacing where the curves deviate from $-4\pi r^2\rho_0$ is within experimental error constant and independent of density.

The changes in the distribution function caused by liquid density are brought into more prominence in Fig. 9 where the normalized distribution functions $4\pi r^2[\rho(r)/\rho_0-1]$ have been plotted. An examination of the curves shows that there is not a uniform change in the form of the first maximum with liquid density. The curves at the lower density 0.095, 0.125, and 0.146 gram/cc recorded along the normal vapor pressure curve[1] show a small change in height together with a

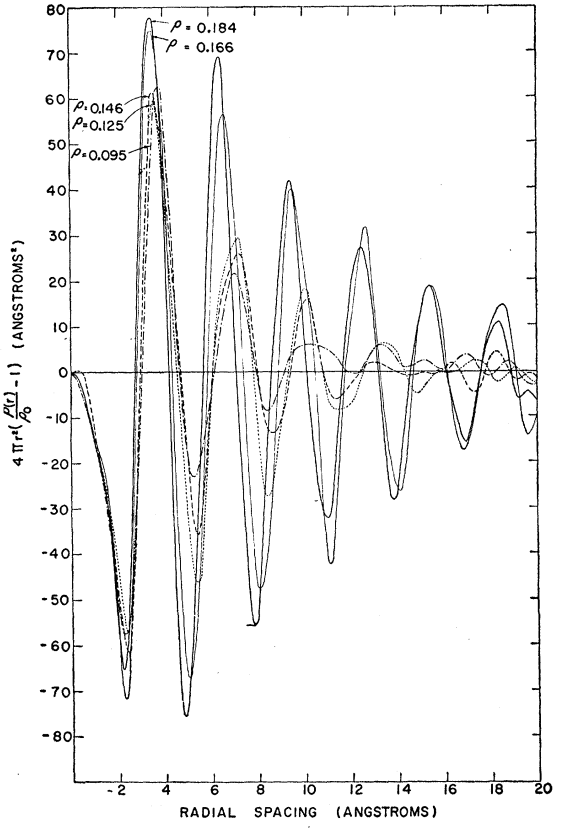

FIG. 9. The normalized transforms $4\pi r^2[\rho(r)/\rho_0-1]$ for each of the transforms of Fig. 8.

slight shift in the maximum to smaller radial spacings while those at the higher density 0.166, and 0.184 gram/cc for pressure above the normal vapor pressure line, show a more marked increase in height together with a shift of the maximum to smaller radial spacings. For all the curves, the amplitude of the second negative maximum increases nearly uniformly with increasing density.

The rate at which the amplitudes of subsequent maxima decrease with increased radial spacing is presumably connected with the long-range order in the liquid. To show how these maxima change with radial spacing, the logarithm of the ratio of the nth peak height

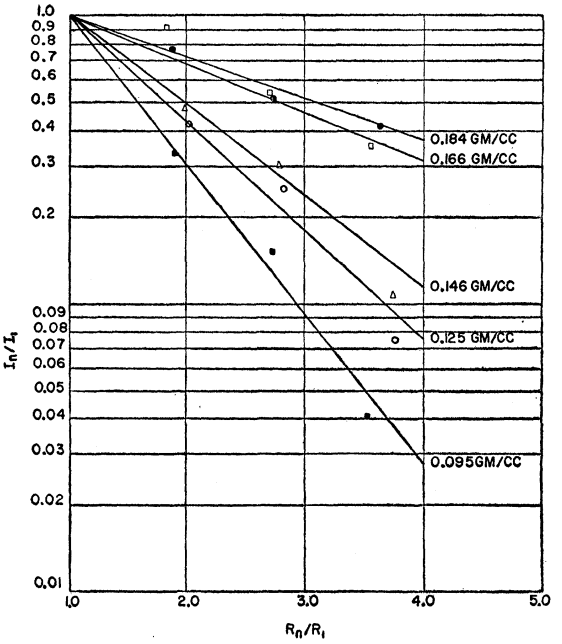

FIG. 10. The rate of decay of the positive maxima of the transforms of Fig. 8. Straight lines have been drawn through the points.

to the first peak height has been plotted in Fig. 10 against the ratio of their spacings. Straight lines have been drawn through the points indicating that to a first approximation, there is an exponential decrease of peak height with radial spacing. The values of the exponent

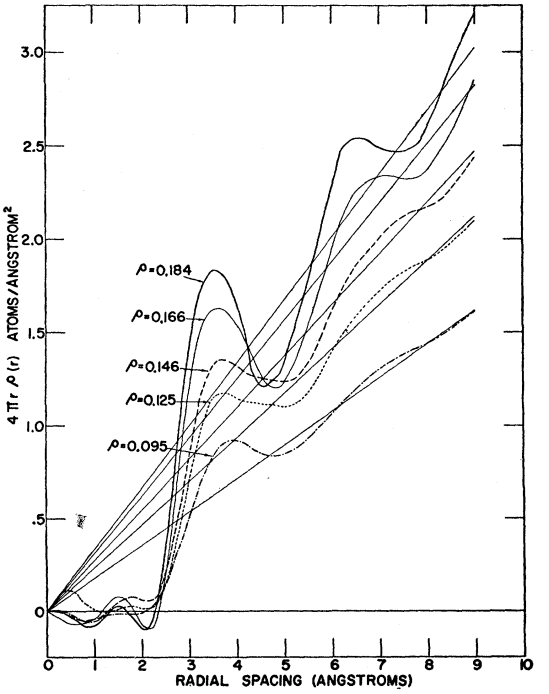

FIG. 11. The radial distribution functions $4\pi r\rho(r)$ for each of the curves of Fig. 8. The straight lines are $4\pi r\rho_0$.

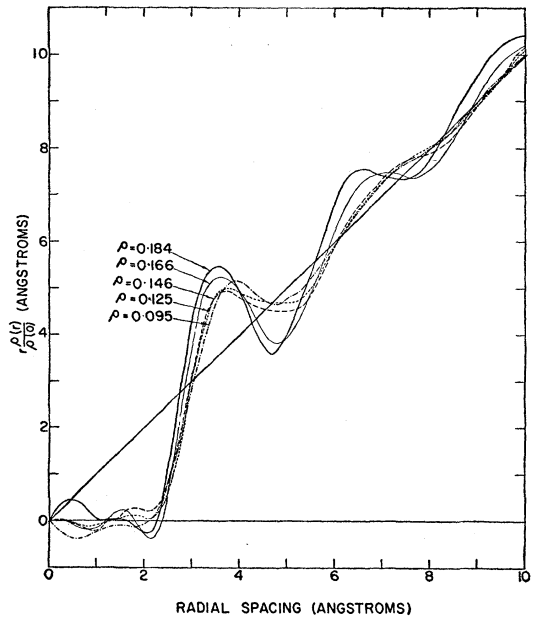

FIG. 12. The normalized radial distribution function $r\rho(r)/\rho_0$ for each of the curves of Fig. 8. The straight line is r.

in the exponential are 1.1_9, 0.8_6, 0.7_2, 0.3_7, and 0.3_3 corresponding to the liquid densities of 0.095, 0.125, 0.146, 0.166, and 0.184 gram/cc, respectively.

The function $4\pi r\rho(r)$ is shown in Fig. 11 for each of the curves of Fig. 8. These curves show an oscillation about zero for spacings out to 2.3 A, a maximum in the region of 3.6 A and an oscillation about $4\pi r\rho_0$ at larger spacings. The effect of increasing liquid density is again seen, the effect of density changes caused by pressure being more pronounced than those caused by temperature along the normal vapor pressure line. The effect of the density changes is brought into more prominence in Fig. 12 where the normalized distribution function $r\rho(r)/\rho_0$ has been plotted for each of the curves. The normalized distribution shows only small changes with liquid density for curves along the normal vapor pressure, the maximum moving to smaller radial spacings and the valley of the first maximum increasing in depth. The changes in the curves produced by pressure are much more marked. Not only is there a marked increase in the height of the main peak together with a shift in the maximum to smaller radial spacings but there is also a marked increase in the depth of the valley following the maximum.

The point where $r\rho(r)$ rises from zero and the position of the first maximum give the nearest distance of approach and the radial spacing of the first shell of atoms. These positions have been determined for all the curves and are listed in Table I and have been plotted as a function of liquid density in Fig. 13. The position where the density rises from zero (lower set of points) changes from a value of 2.2 A at 0.095 gram/cc to a maximum of 2.35 A in the region of 0.17 gram/cc. Thus this value is within experimental error constant and independent of density giving the nearest distance of approach of 2 atoms in the liquids as 2.27±0.08 A. The position of the maximum in $r\rho(r)$ (upper set of points) decreases with increasing density showing that there is a change in the mean radius of the first coordinate shell. The full curve represents the expected decrease for a uniform dilation of a basic structure. The experimental points do not fall on the theoretical curve, again indicating that such a simple model will not explain the density changes.

The number of neighbors under the first shell of atoms has been determined for each of the curves using two methods.[1] The first was a determination of the number of neighbors under a peak symmetrical in $4\pi r\rho(r)$ about the maximum in $4\pi r\rho(r)$ while the second was a peak

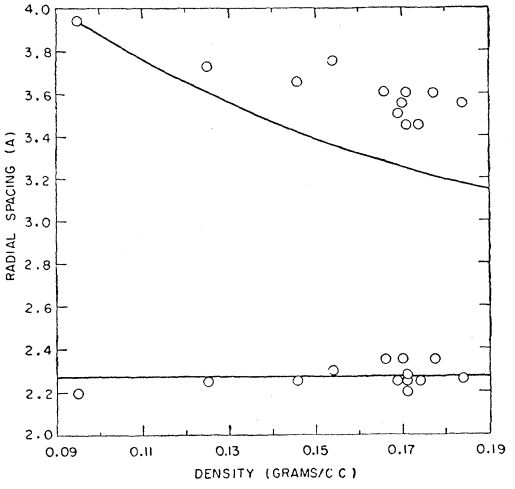

FIG. 13. The position where $r\rho(r)$ rises from zero and its maximum as a function of liquid density. The upper smooth curve represents the expected variation of the position of the maximum as a function of liquid density assuming a uniform dilation of a basic structure. The points do not fit the theoretical curve. The lower horizontal line represents the average value of the position of the zero.

symmetrical in $4\pi r^2\rho(r)$ about the maximum in $4\pi r\rho(r)$. The number of neighbors under the second shell of atoms assuming peaks symmetrical in $4\pi r\rho(r)$ has also been calculated.[1] The results are listed in Table I. The number of neighbors calculated by the first method gave values about 1.2 atoms greater than the number calculated by the second. These results have been plotted as a function of liquid density in Fig. 14, in which the squares represent the number of second neighbors, the open circles and closed circles the number of first neighbors calculated by the first and second method, respectively. Smooth curves have been drawn through the points. The horizontal dotted line represents the number of neighbors under the first shell of atoms at the freezing point if the density change (7%) during the solid-liquid transformation were caused by a uniform

depletion of atoms from a basic structure in the close packed solid.[16]

The measured ratio of the spacings of the second to first coordinate shell has values 1.38, 1.36, 1.40_5, 1.40_4, and 1.47_5 corresponding to liquid densities of 0.184, 0.166, 0.146, 0.125, and 0.095 gram/cc, respectively. These values are not markedly different from the value $\sqrt{2}=1.414$, the value expected for a close-packed configuration. Thus the ratio of spacings of second to first neighbors decreases slightly with increasing density but has values close to that expected on the basis of a close-packed structure. The corresponding ratio of the numbers of first to second neighbors changes rapidly from a value of 0.7_2 to 1.5_5 for densities changing from 0.095 gram/cc to 0.184 gram/cc and tends to approach the value 2 expected for a close-packed configuration. Thus the liquid is tending to form a close-packed array at higher liquid densities.

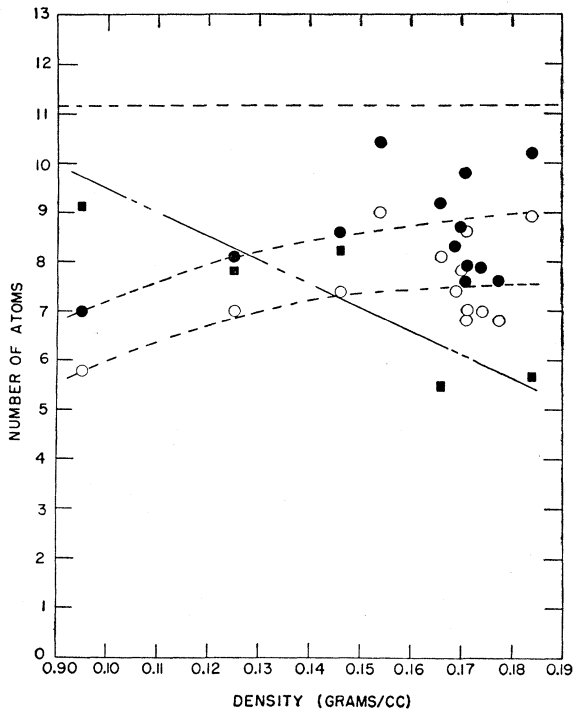

FIG. 14. The open and closed circles represent the number of neighbors under the first shell of atoms. The dotted curves were drawn as guides to the eye. The closed squares represent the number of neighbors under the second shell of atoms. The broken line was drawn through these points as a guide to the eye. The upper dotted line is the theoretical number of neighbors under the first shell of atoms if the solid-liquid transformation were due to a uniform depletion of atoms from a uniform structure. The experimental points fall below the theoretical curve.

The number of neighbors under the first shell of atoms at a temperature of 1.9°K and a pressure close to the freezing line is about 8.5 atoms. This number is 29% less than the number in a hexagonal close-packed structure[16] and shows that the 7% change in liquid density cannot be accounted for by a uniform dilation of atoms in a close-packed structure but that there must be a reorganization of atoms during the solid liquid transformation.

[16] D. G. Henshaw, Phys. Rev. **109**, 328 (1958).

ACKNOWLEDGMENTS

Thanks are due to Dr. B. N. Brockhouse, Dr. D. G. Hurst, and Dr. N. K. Pope for helpful discussions and to J. R. Freeborn for technical assistance.

APPENDIX I

The calculation of the effect of a uniform dilation of a basic structure on the form of the scattering pattern is as follows:

The formula connecting the normalized intensity $i(s)$, with the atomic density distribution $\rho(r)$ is

$$si(s)=\int_0^\infty 4\pi r[\rho(r)-\rho_0]\sin(sr)dr.$$

For a uniform dilation in which all distances are increased by a factor ϵ, we may write

$$r'=\epsilon r,$$
$$\rho_0'=(1/\epsilon^3)\rho_0.$$

Then

$$s'i(s')=\int_0^\infty 4\pi r[\rho'(r)-\rho_0']\sin(s'r)dr.$$

Since the integration extends from 0 to ∞, we can replace r by r':

$$s'i(s')=\int_0^\infty 4\pi r'[\rho'(r')-\rho_0']\sin(s'r')dr'.$$

Now put $\rho'(r')=(1/\epsilon^3)\rho(r)$ and $r'=\epsilon r$, whence

$$s'i(s')=\int_0^\infty 4\pi\epsilon r\frac{[\rho(r)-\rho_0]}{\epsilon^3}\sin(s'\epsilon r)d\epsilon r$$
$$=\frac{1}{\epsilon}\int_0^\infty 4\pi r[\rho(r)-\rho_0]\sin(\epsilon s'r)dr.$$

Thus the value $s'i(s')$ at $s'=(1/\epsilon)s$ is exactly $1/\epsilon$ times the value of $si(s)$ at s. In particular,

(i) the height of the maximum of $(2/\pi)s'i(s')$ $=(\rho'/\rho)^{\frac{1}{3}}\times$maximum of $(2/\pi)si(s)$;
(ii) the value of $(s')_{\max}=(\rho'/\rho)^{\frac{1}{3}}\times$value of $s_{\max}$;
(iii) the position $s'_{(\text{zero})}=(\rho'/\rho)^{\frac{1}{3}}\times$value of $s_{(\text{zero})}$.